Springer

KSME

Journal of Mechanical Science and Technology 33 (11) (2019) 5337~5346
www.springerlink.com/content/1738-494x(Print)/1976-3824(Online)
DOI 10.1007/s12206-019-1026-2

Optimization of process parameters to enhance formability of AA 5182 alloy in deep drawing of square cups by hydroforming †

Bharatkumar Modi and D. Ravi Kumar*

Department of Mechanical Engineering, Indian Institute of Technology Delhi, India

(Manuscript Received October 29, 2018; Revised June 12, 2019; Accepted August 22, 2019)

Abstract

The formability of 1 mm thick AA5182 aluminum alloy sheets in deep drawing of square cups by hydroforming was studied. The influence of process parameters (peak pressure, pressure path, and blank holding force) on formability was investigated through numerical simulations and validated with experimental work. The experiments were designed using the Taguchi method. The minimum thickness in the formed cups (at the bottom corners) and the minimum corner radius that can be achieved were considered as the criteria for evaluation of formability. The peak pressure was the most important process parameter affecting thinning and the minimum corner radius that can be achieved. The variation of the pressure path had the least effect on formability. Regression models were developed for prediction of minimum thickness in the cup and the corner radius as a function of peak pressure and blank holding force.

Keywords: Aluminum alloy; Deep drawing; Formability; Hydroforming

1. Introduction

The importance of sheet metal forming processes with the assistance of fluid pressure has increased significantly due to certain advantages of these processes over conventional sheet metal forming processes [1-3]. High pressure fluid is applied on the blank usually through the blank holder to form it into the shape of the die cavity, as shown in Fig. 1. The mechanism of sheet hydroforming was explained by Hein and Vollertsen [4].

Sheet hydroforming, in general, has a large potential to produce auto body components with consistently high levels of tensile strength and rigidity, optimized weight, accurate geometry, and close tolerances. It has advantages like more uniform thickness distribution in the component, lower tooling cost and use of modular dies to make parts of different geometry with the same setup. Better surface finish can be achieved as thin film lubrication takes place between blank and blank holder due to the presence of fluid. Trial runs and batch production is quite economical as dies from concrete, wood or polyurethane can also be used [5]. A single die setup can be used for any thickness of blank material, as no mating punch is required. Forming of two parts in a single setup as well as a welded hollow assembly is quite possible [3, 4, 6]. Also, hydroforming can produce complex single body geometries with high structural stiffness, which using conventional forming methods can only be produced in multiple, welded components like body and suspension parts [7, 8]. Thus, hydroforming leads to a completely new category of sheet metal formed parts, made of sophisticated materials, produced in only one manufacturing process, offering new prospects for lightweight constructions and cheaper products.

Successful production of parts using hydroforming mainly depends on design aspects of tooling as well as control of important process parameters such as closing force or blank holding force and fluid pressure. However, due to larger process variables when compared to conventional deep drawing, accurate process control is difficult in hydroforming. Therefore, sheet hydroforming is still being investigated for its overall suitability for commercial production. Erkan and Erman [9] carried out a comparative study of high pressure sheet metal forming, hydro-mechanical deep drawing and conventional deep drawing on workpieces with various cross-sections. Working windows for each process were established based on the parameters of the circular, elliptic, rectangular and square cross-sectional product geometries with ultralow carbon steel.

Desai and Date [10] quantified the effect of material, tool and process parameters on strain distribution in the drawn sheet metal components. Higher and more uniform strain-hardening with an expected reduction in spring-back due to the introduction of hydrostatic pressure was illustrated by Yang et al. [11]. Manufacturability of micro-channels in a

*Corresponding author. Tel.: +91 11 26591144
E-mail address: dravi@mech.iitd.ac.in
† Recommended by Associate Editor Young Whan Park

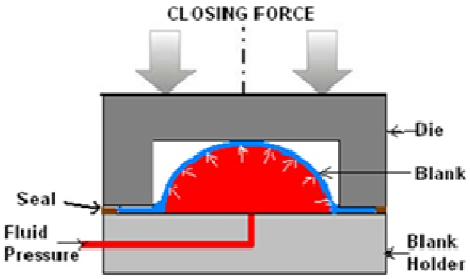

Fig. 1. A schematic diagram for hydroforming of flat bottom cup-shaped components.

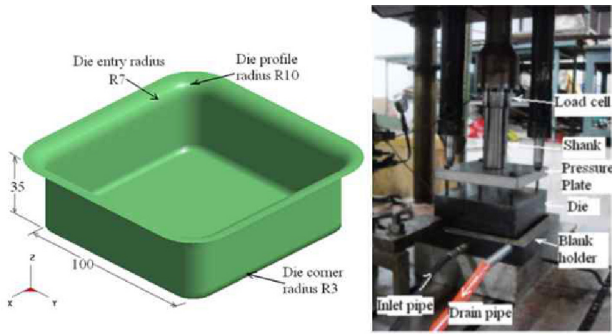

Fig. 2. Dimensions of the die (in mm) and the experimental setup [32].

bipolar plate of a fuel cell and a funnel shape was studied by Sasawat and Koc [12] and Hojjati et al. [13], respectively, to evaluate the effects of applied pressure on important formability parameters such as thickness distribution, final dome height, and distributions of equivalent stress and strain. To increase the formability of structural parts having a shape like that of an oil pan, Kim et al. [14] proposed a multi-stage hydro-forming process of a sheet pair in which thinning was reduced by more than 30 %. With the same aim, Shi-Hong et al. [15] also studied sheet hydroforming process with a movable female die which was kept in contact with the deformed area of the sheet blank so that further deformation of the deformed area was restricted, and it resulted in less thinning than in the hydro bulged part and remarkably improved limiting draw ratio of stainless steel-SS304.

The role of surface roughness and friction (with or without lubrication) was extensively studied in the case of conventional sheet metal forming [16-18], but in sheet hydroforming, it was reported only by a few researchers. It was found that sheet surface frequently becomes rougher with increasing plastic strain if surface defects like tool marks are present before hydroforming of a blank [19]. Higher accuracy and surface finish were found in sheet hydroforming when compared to conventional deep drawing for the production of an automobile fuel tank [20]. Shin et al. [21] discussed the welded blank hydroforming technology in the formability of the engine mount bracket and the subframe. Kreis and Hein [22] presented an integrated approach to shorten the process chain for the manufacturing of complex hollow bodies made of sheet metal by developing a manufacturing system that integrates the process steps: Hydroforming, mechanical trimming, laser beam welding, and hydro-calibrating.

The control of the blank holding force (BHF) plays an important role in the success of the hydroforming process. Geiger et al. [23] Novotny and Hein [6] developed pressure-BHF process windows for successful hydroforming of sheet pairs with extra-low carbon steel (DC04) and aluminum alloy (AA6016) materials in which forming was carried out in two steps, preforming and calibration. Improvement in formability has also been reported by Liu et al. [24] with the stepped-BHF load path. Peter and Matin [25] proposed an active elastic tool and a leakage detection CCD-camera system for pressure-BHF load path control. A bursting pressure limit was extended, and as a result, the formability of DC04 material was improved. Halkaci et al. [26] showed that formability could be enhanced by adding a shallow draw bead to the blank holder in the hydro-mechanical deep drawing process. Several researchers have conducted analytical studies of the high pressure bulge hydroforming process. Elkholy and Al-Hawaj [27] analyzed stresses developed and collapse pressure for a simply supported and rigidly supported circular plate of an elastic-perfectly plastic material. An artificial intelligence technique known as neural networks and random neural networks (RNNs) was developed by Karkoub [28] to predict the amount of deformation caused by high pressure hydroforming. Ahmad and Mohammad [29] proposed an upper bound method to estimate pressure required for hydroforming of sheet metal pairs. A hemispherical part was formed to validate the effect of the parameters like work-hardening exponent, friction and blank size.

Sheet hydroforming is especially suitable for light-weight materials like aluminum alloys which have low formability in conventional forming processes. AA5182 and AA5754 aluminum alloys were characterized and the mechanical properties were found suitable for deep drawing [30, 31]. Limited literature is available to estimate formability under different pressure-BHF load path conditions for hydroforming of aluminum alloys. The analytical study was limited only to the prediction of bulge height under the applied pressure. In view of this, in the present work, an experimental and numerical study was carried out on the influence of process parameters on formability in deep drawing of square cups by hydroforming from AA5182 alloy sheet and these parameters have been optimized to maximize formability using Taguchi method.

2. Experimental work

2.1 Experimental setup

An experimental setup was designed and developed for deep drawing of square cup-shaped parts by hydroforming of sheets in the thickness range of 0.5 mm to 1.4 mm. The dimensions of the die designed for hydroforming of square cups and the experimental setup on a hydraulic press are shown in

Table 1. Mechanical properties and anisotropic parameters of AA5182 sheets.

Angle with respect to rolling direction (°)	YS (MPa)	UTS (MPa)	% Elongation	Strain hardening exponent n	Strength coefficient K (MPa)	Anisotropic parameter R
0	161.8	295.0	18.0	0.35	635.1	0.75
45	145.3	273.0	19.6	0.36	577.2	0.90
90	157.5	283.8	18.8	0.35	589.4	0.82
Average	152.5	281.2	19.0	0.35	594.8	0.84 ($\bar{R}$)
Standard deviation	8.5	11.0	0.8	0.004	30.5	0.08

Fig. 2. The complete details of the development of the experimental setup and the controls along with a data acquisition system have already been published [32].

2.2 Composition and mechanical properties

AA5182 alloy, used in the present study, is a non-heat treatable Al-Mg alloy containing 4.3 % Mg, 0.34 % Mn and 0.21 % Fe. The mechanical properties and anisotropic parameters of 1 mm thick AA5182 alloy sheets in the annealed condition (O-temper) are listed in Table 1.

2.3 Design of experiments

Design of experiments (DOE) techniques like the Taguchi method and response surface methodology are used to optimize the process parameters by minimizing the number of experiments. A large number of researchers [33-35] demonstrated the effectiveness of these methods to determine the optimal parameters for various sheet metal forming processes. Experiments were designed using the Taguchi DOE technique to study the effect of process parameters (pressure path, peak pressure, and BHF) on the formability of AA5182 alloy in hydroforming of square cups. In addition to these three variables, friction at blank-tool interfaces also has a significant effect on formability. The value of the friction coefficient depends on the prevailing condition at the interface (presence/absence of lubrication and the type of lubricant) and it is not a process parameter which can be controlled directly, and hence it is excluded from the parametric study. However, the effect of friction and lubrication on overall formability in hydroforming was reported by Modi and Kumar [36].

2.3.1 Levels of process parameters

From the preliminary experiments, it was observed that the pressure required just to bulge the material up to the full depth of the cavity is 10 MPa, and on further increase in pressure the magnitude of form filling increases. The maximum pressure the material can sustain was found to be 24 MPa. So, three levels of peak pressure were chosen with the initial level of 14.5 MPa to have considerable form filling, 19.0 MPa as an intermediate level and 23.5 MPa as the highest level just below the maximum possible pressure.

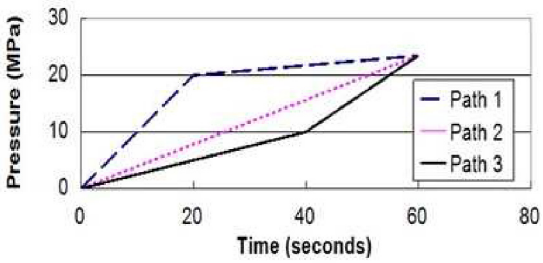

Fig. 3. Different pressure paths used in hydroforming experiments.

Three pressure paths as shown in Fig. 3 were considered for the study and the total cycle time was the same in all the three cases. In pressure path 1, the pressure was linearly increased to 20 MPa (just below the peak pressure) in 25 seconds (forming stage) and was then gradually increased during the remaining part of the total cycle time of 60 seconds (calibration). The pressure was continuously increased to peak pressure in 60 seconds in pressure path 2. In pressure path 3, a pressure of 10 MPa was reached in 40 seconds, and it was then increased to the peak pressure at a faster rate during calibration.

The minimum closing force or sealing force found from the experiments was just above the upward force, i.e., static equilibrium force due to fluid pressure in the die cavity. It prevents leakage of the fluid and ensures pressure development in the die cavity. Estimation of closing force and its variation during the cycle was explained in earlier work [32].

The applied blank holding force (BHF), i.e., force above the minimum closing force, affects forming modes (the extent of drawing/stretching and thinning). Three levels of BHF- 10 kN, 20 kN and 30 kN (in addition to the minimum closing force) were chosen to capture its effect on hydroforming. Three experiments were carried out for each set of variables. MINITAB software was used for statistical analysis of the Taguchi DOE technique.

2.3.2 Contribution of process parameters on minimum thickness and radius at the corner

Taguchi analysis was carried out for minimum thickness and radius at the corner (mean values) in the hydroformed cups. Greater the better criterion was chosen for thickness analysis, as higher thickness at corner indicates lower thinning and better formability. Smaller the better criterion was chosen for corner radius as a lower corner radius means better form filling and higher geometrical accuracy.

The signal to noise (S/N) ratio was used to measure the deviation of responses (thickness and radius). The S/N ratio is expressed [37] as:

$$S/N\,ratio = -10\log\left(MSD\right) \tag{1}$$

where MSD is the mean square deviation of the responses.

$$MSD = \frac{1}{n}\left(\sum_{i=1}^{n}\left(\frac{1}{Y_i}\right)^2\right) \quad \text{for larger the better criterion} \tag{2}$$

$$MSD = \frac{1}{n}\left(\sum_{i=1}^{n}(Y_i)^2\right) \quad \text{for smaller the better criterion} \tag{3}$$

where n is the number of experiments and Y is the measured value of responses.

The overall mean S/N ratio is expressed as:

$$\overline{S/N} = \frac{1}{9}\left(\sum_{i=1}^{9}(S/N)_i\right) \tag{4}$$

The sum of squares (SS) due to variation about the overall mean is:

$$SS = \sum_{i=1}^{9}\left((S/N)_i - \overline{S/N}\right)^2 \tag{5}$$

For the i^{th} process parameter, the sum of squares due to variation about the mean is:

$$SS_i = \sum_{j=1}^{3}\left((S/N)_{ij} - \overline{S/N}\right)^2 \tag{6}$$

The percentage contribution of individual process parameter on the responses can be calculated by:

$$\%\ Contribution_i = \frac{SS_i}{SS} \times 100\ . \tag{7}$$

2.4 Measurement of output and analysis

2.4.1 Measurement of blank holding force and fluid pressure

Blank holding force was sensed through a 50-ton capacity load cell, which was attached with the press ram. A pressure gauge and a pressure transducer were installed at the input line of the die setup to measure and record the fluid pressure exerted on the blank. Data acquisition system was used to acquire load and pressure data.

2.4.2 Measurement of strain, thickness, and corner radius

Before performing the experiments, the blank surface was marked with a 5 mm diameter circle grid with laser marking technique for the strain measurement. The circle deforms into an ellipse due to the deformation of the blank into the die cavity shape. The major and minor diameters of the deformed circles (ellipses) were measured by a traveling microscope with a least count of 0.001 mm to obtain major and minor strains in different regions. To study the thickness variation in the hydroformed cups, the thickness was measured at different points along the face and the diagonal of the cup bottom at an interval of 5 mm by using a pointed anvil micrometer of 0.01 mm least count. For the measurement of corner radius, a coordinate measuring machine was used. The thickness and the corner radius were measured for all the cups drawn with different combinations of process variables.

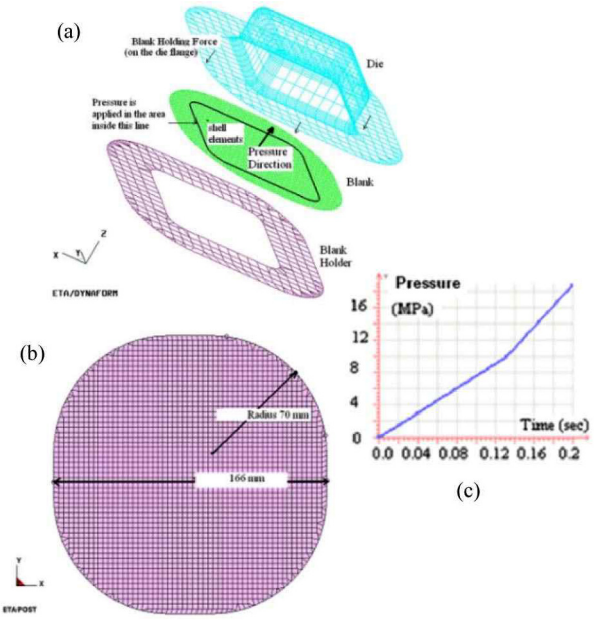

Fig. 4. (a) FE model used for simulation of hydroforming of square cups; (b) initial blank; (c) a typical pressure path.

3. Numerical simulation methodology

Hydroforming of square cups was modeled and simulated using the finite element method with the help of commercially available software Dynaform with LS-DYNA (version 971) to arrive at a suitable range of process parameters and evaluate their influence on formability of AA5182 alloy. The tools (die and blank holder) and the blank were created by surface modeling. In the present work, triangular and rectangular thin shell elements were used with an average element size of 3 mm. Tools were modeled as rigid bodies, neglecting very little elastic deformation of the tools during deep drawing. A typical FE model of the tools and the blank used for simulation of sheet hydroforming of a 35 mm deep square cup is shown in Fig. 4(a). A 1 mm thick square blank of 166 mm side with a corner radius of 70 mm (Fig. 4(b)) was modeled with five integration points through the thickness using the Gauss rule.

3.1 Material model

To represent the yielding behavior of AA5182 alloys in FEA accurately, Barlat's 1989 3-parameter yield model was used. Barlat's model incorporates the effect of both normal and planar anisotropy in a polycrystalline sheet during plastic deformation [38]. This represents the material behavior in close approximation to experimental behavior. Tensile properties and anisotropic parameters of the alloy, determined from

the tensile tests were given as input to define the material behavior during plastic deformation.

3.2 Boundary conditions

The required boundary conditions were defined in the simulation of hydroforming of square cups. Blank was defined as the master surface and the dies were defined as slave surfaces. The friction conditions were modeled using Coulomb friction at the blank-tool interfaces. The friction condition at blank-blank holder interface was approximated as semi-fluid film lubrication under the influence of fluid pressure and coefficient of friction was taken to be 0.08 as suggested by Rao and Xie [39]. The coefficient of friction at the contact between the blank and the die (without lubrication) was taken as 0.3 (for dry condition) [40]. The lubricated condition with Teflon was modeled with the value of the coefficient of friction as 0.04 [32]. Pressure boundary condition was applied at all the nodes on the blank within the area confined by a line as shown in Fig. 4(a), and the enclosed area represents the region in which the fluid pressure was applied on the blank. A typical pressure path defined as an input in the FE simulation of hydroforming is shown in Fig. 4(c).

4. Results and discussion

4.1 Effect of process parameters

Some important results obtained from numerical and experimental work on hydroforming of square cups are presented in this section. A square cup that was hydroformed with pressure path 1, peak pressure 14.5 MPa and BHF 10 kN is shown in Fig. 5, and the measured thickness distributions along the face and diagonal directions in the cup are also shown.

The minimum thickness (0.88 mm) was observed at the corner in the diagonal direction from the center of the bottom. FE simulation result (Fig. 6) showed that the predicted major and minor strains were well below the FLD, which means the cup can be formed successfully with these parameters without any risk of necking or failure, which is in agreement with experimental observation. The thickness distribution in the component predicted in the FE simulation is also shown in Fig. 6. The maximum thinning occurred at the four bottom corners of the cup, and hence the minimum thickness was observed at the corner when measured along the diagonal. The corner radius that could be achieved experimentally with these parameters is 42.7 mm and with FE simulation, it is 39.07 mm as shown in Fig. 9 indicating that the experimental and FE simulation results are in good agreement. However, the corner radius achieved with these parameters is much higher than the desired corner radius.

With the combination of process parameters listed at experiment number 6 in Table 2 (peak pressure 23.5 MPa, BHF 10 KN and pressure path 2), the component could be successfully hydroformed. The minimum thickness achieved at the

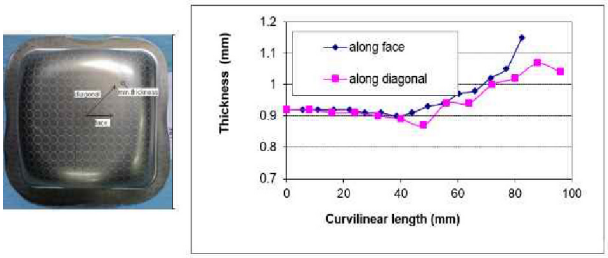

Fig. 5. Experimentally formed cup and thickness variation along the face and the diagonal with pressure path 1, peak pressure 14.5 MPa and BHF 10 kN.

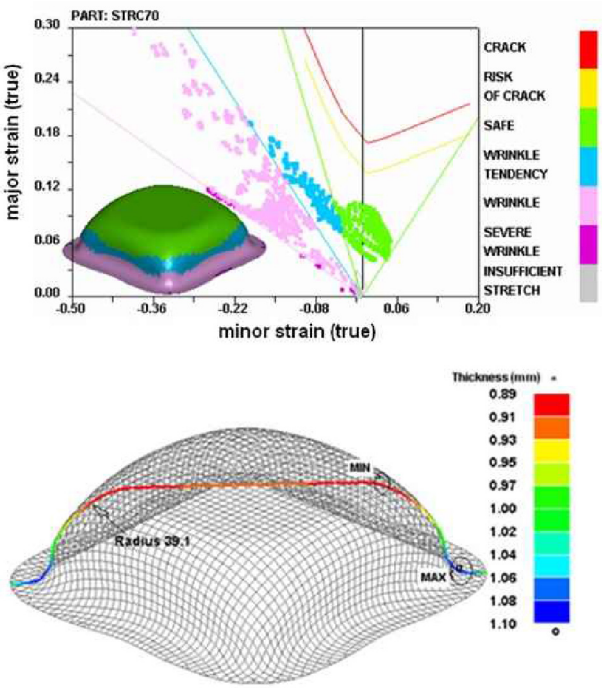

Fig. 6. Formability prediction and thickness variation in FE simulation of square cup hydroforming (pressure path-1, peak pressure 14.5 MPa and BHF 10 kN).

corners with experiments and FE simulations is 0.80 mm and 0.82 mm, respectively. The thickness variation in the component, obtained from FE simulations, is shown in Fig. 7. The corner radius that could be achieved experimentally with these parameters is 26.3 mm, and this is in good agreement with the corner radius predicted by FE simulations, which is 22.93 mm, as represented in Fig. 7. It can be observed from the results that higher thinning was obtained at the corner due to higher fluid pressure when compared to the case discussed earlier with pressure path-1. In this case, the fluid pressure continuously increased till the end leading to more biaxial stretching at the corner towards the end.

Accordingly, a much lower corner radius was achieved due to larger deformation in the corner region. Major and minor strains at the corner almost reached the highest allowed safe strains, as shown by the yellow line in the FLD (Fig. 7).

A hydroformed square cup with the process parameters of

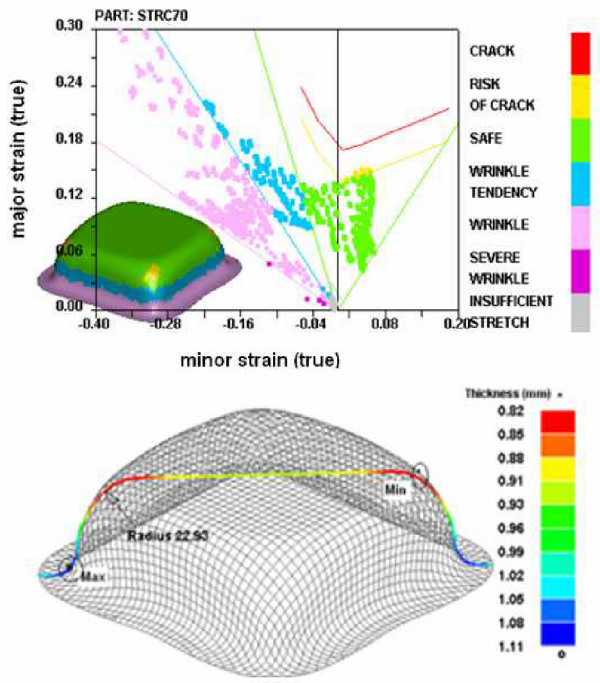

Fig. 7. Formability prediction and thickness variation in FE simulation of square cup hydroforming (pressure path-2, peak pressure 23.5 MPa and BHF 10 kN).

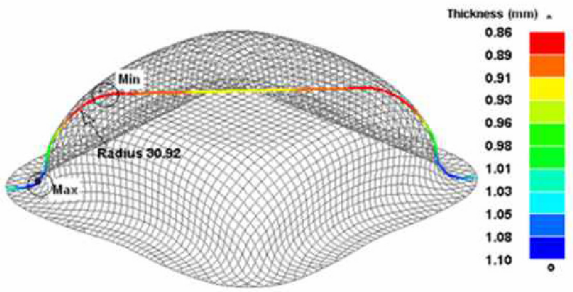

Fig. 8. Thickness variation and corner radius prediction in FE simulation with pressure path 3, peak pressure 19.0 MPa and BHF 10 kN.

experiment number 8 (pressure path 3, peak pressure 19 MPa and BHF 10 KN) is shown in Fig. 8. The success of the cup was also predicted from the FE simulations. The minimum thickness achieved at the corners with experiments and FE simulation was 0.85 mm and 0.86 mm, respectively. The thickness variation in the FE simulation is shown in Fig. 8. The corner radius that could be achieved experimentally with these parameters was 33.4 mm and it was 30.92 mm in FE simulation as shown in Fig. 8.

Though the pressure rapidly increased in the calibration stage in pressure path-3, the thinning in the corners was less than the previous case due to lower peak pressure, and hence the formed corner radius is higher.

4.2 Failure in hydroforming of square cups

The components were successfully hydroformed with all

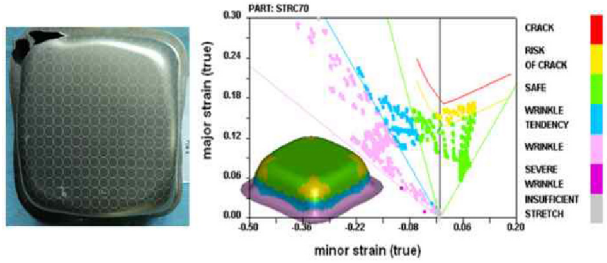

(a) (b)

Fig. 9. Failure in the hydroformed cup (pressure path 1, peak pressure 23.5 MPa and BHF 30 kN): (a) Experimentally formed cup; (b) formability prediction in FE simulation.

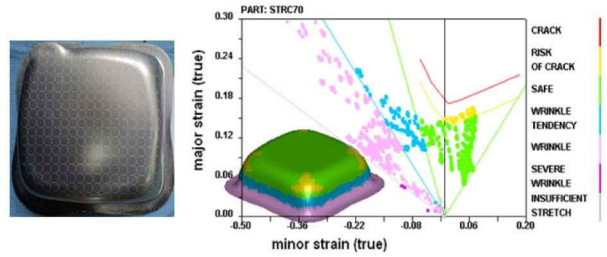

(a) (b)

Fig. 10. Failure in the hydroformed cup (pressure path 3, peak pressure 23.5 MPa and BHF 20 kN): (a) Experimentally formed cup; (b) formability prediction in FE simulation.

sets of parameters as per the DOE (Table 2), except in the case of pressure path 1 (experiment 3) and pressure path 3 (experiment 9) with a peak pressure of 23.5 MPa. The minimum thickness achieved at the corner in experiment 3 and experiment 9 was 0.76 mm and 0.77 mm, respectively. The failure in the cups formed in the experiments was found in the corners and the cups are shown in Figs. 9(a) and 10(a). The strains predicted in FE simulations are also in risk of failure zone as seen in Figs. 9(b) and 10(b), and hence the predicted results are consistent with experimental findings. The failure is due to higher fluid pressure and higher BHF than in the cases discussed earlier. Higher BHF causes a higher constraint on the material flow during initial stages of draw-in, and hence the stretching component increases, leading to more thinning. Therefore, the material is unable to undergo further deformation in the corners during calibration under high fluid pressure, and hence a fracture occurs at the corner.

4.3 Main effects plot for minimum thickness

Taguchi analysis was carried out for minimum thickness and radius at the corner of the cups from experiments and FE simulations. Minimum cup wall thickness (in the corner region) and radius at the cup corner were chosen as responses of the Taguchi experiments. The responses from experiments and FE simulations are tabulated in Table 2.

For each combination of process parameters, three experiments were carried out and the average values (maximum

Table 2. Experimental layout and responses.

Exp no.	Pressure path	Peak pressure (MPa)	BHF (kN)	Min. thickness (mm)		Min. corner radius (mm)	
				Exp.	FEA	Exp.	FEA
1	1	14.5	10	0.89	0.89	43.1	39.1
2	1	19.0	20	0.84	0.84	33.2	30.1
3	1	23.5	30	0.76	0.77	27.3	24.2
4	2	14.5	20	0.90	0.88	40.7	37.8
5	2	19.0	30	0.82	0.83	29.7	25.9
6	2	23.5	10	0.80	0.82	26.0	22.9
7	3	14.5	30	0.86	0.86	42.8	40.1
8	3	19.0	10	0.85	0.86	33.3	30.9
9	3	23.5	20	0.77	0.79	27.6	24.1

standard deviation for thickness is 0.01 mm and for corner radius, it is 1.3 mm) were reported. The results predicted by FE simulations were also compared with the experimental results. 'Greater the better' criterion was chosen as higher thickness at the corner indicates lower thinning and better formability. The plots of the main effects are shown in Figs. 11(a) and (b) for the minimum thickness observed at the cup corner in the experiments and FE simulations, respectively.

Mean values of thickness achieved experimentally at different levels of process parameters are also listed in Table 3. 'Delta' represents total variation in mean thickness caused by the change in the level of individual process parameters. The process parameter (peak pressure) with the highest value of 'Delta' was ranked one, and it has the highest influence on the response (thickness) among all the parameters. BHF was found to be the next influential parameter with rank 2, and the pressure path had the least effect among all the process parameters. The contribution of each parameter was also worked out and these results are also presented in Table 3.

4.4 Prediction of minimum thickness by regression analysis

Using the Taguchi analysis of the experimental results, a regression equation for 'minimum thickness' was proposed (Eq. (8)). It predicts the minimum thickness as a function of the process parameters within the range used in the study. The parameter 'pressure path' was not included in the equation as it does not have a numerical value. The fitness of the equation was found to be 93.9 % from the analysis of variance.

$$\text{Minimum thickness (mm)} = 1.09 - 0.0117 * \text{Peak Pressure} - 0.00161 * \text{BHF} \quad (8)$$

where peak pressure is in MPa and BHF is in kN.

4.5 Main effects plot for the corner radius

Smaller the better criterion was chosen for the response 'corner radius' as lower the radius, better the form filling and hence higher geometrical accuracy of the formed part. The plots of the main effects are shown in Figs. 12(a) and (b) for cup corner radius obtained through experiments and FE simulations respectively. The mean values of the corner radius that can be achieved experimentally at different levels of process parameters are also listed in Table 4. The process parameter (peak pressure) with the highest value of 'Delta' was ranked one and it had the highest influence on the response (corner radius) among all the parameters. Pressure path was found to be the next influential parameter with rank 2 and BHF had the least effect among all the process parameters. The contributions of each parameter are also presented in Table 4.

Table 3. Response table for means (thickness) and contribution of process parameters.

Level	Pr. path	Peak Pr. (MPa)	BHF (kN)
1	0.8300	0.8833	0.8467
2	0.8400	0.8356	0.8356
3	0.8267	0.7778	0.8144
Delta	0.0133	0.1056	0.0322
Rank	3	1	2
SS	0.011	0.617	0.059
% contribution	1.56	89.81	8.63

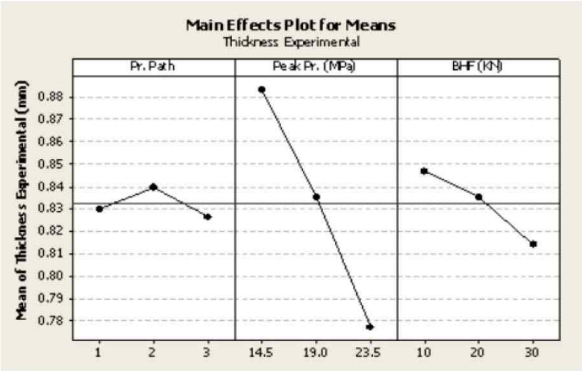

(a)

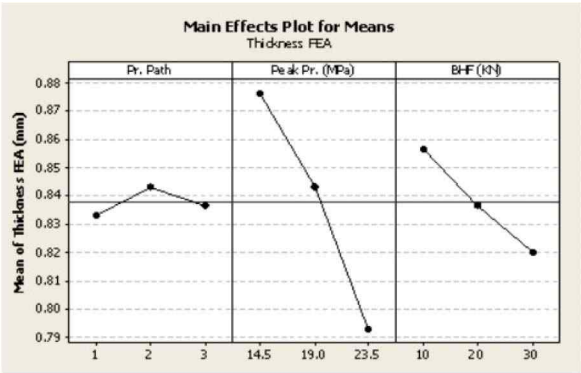

(b)

Fig. 11. Main effects plot for minimum thickness obtained from (a) experimental results; (b) FEA results.

Table 4. Response table for means (corner radius) and contribution of process parameters.

Level	Pr. path	Peak Pr. (MPa)	BHF (kN)
1	34.47	42.20	34.14
2	32.07	32.03	33.81
3	34.57	26.87	33.14
Delta	2.50	15.33	1.00
Rank	2	1	3
SS	0.992	30.832	0.138
% contribution	3.11	96.46	0.43

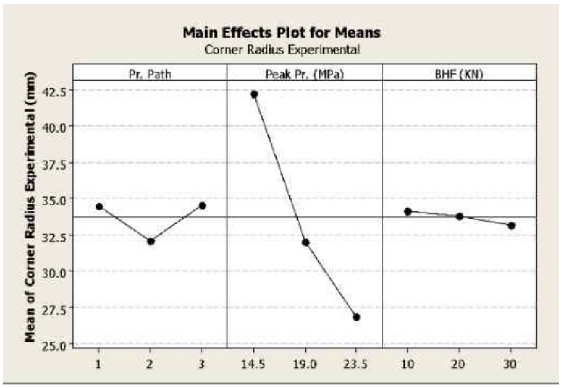

(a)

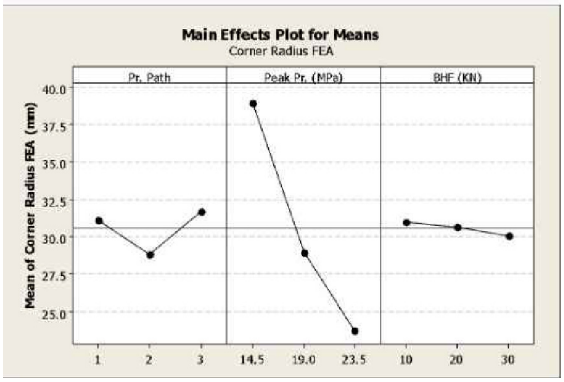

(b)

Fig. 12. Main effects plot for corner radius obtained from (a) experimental results; (b) FEA results.

4.6 Prediction of corner radius by regression analysis

Using the Taguchi analysis of the experimental results, a regression equation for 'corner radius' was proposed (Eq. (9)). It predicts the minimum corner radius as a function of the process parameters within the range used in the study. As mentioned earlier, the parameter 'pressure path' was not included in the equation as it does not have a numerical value. The fitness of the equation was 91.8 % from the analysis of variance.

$$\text{Corner radius (mm)} = 67.1 - 1.70 \text{ peak pressure} - 0.0500 \text{ BHF} \quad (9)$$

Table 5. Comparison of the results predicted from regression models and the experimental work.

Optimum process parameters	For minimum thinning		For minimum corner radius	
Pressure path	2		2	
Peak pressure (MPa)	14.5		23.5	
BHF (KN)	10		30	
Responses	Regression	Exp.	Regression	Exp.
Min. thickness (mm)	0.91	0.91	0.77	0.78
Corner radius (mm)	41.0	44.0	24.7	25.6

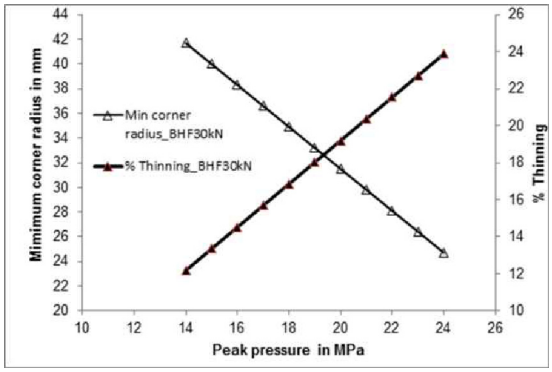

Fig. 13. Influence of peak pressure on thinning and corner radius predicted by regression equations.

where peak pressure is in MPa and BHF is in kN.

As the peak pressure is the most influential process parameter on formability, variations of % thinning and corner radius predicted using Eqs. (8) and (9), respectively, for different values of peak pressure are shown in Fig. 13. For a given value of BHF, as the peak pressure increases, percentage thinning increases and the achievable minimum corner radius decreases.

However, while it is important to be able to form small corner radii in sheet metal forming, the percentage thinning cannot exceed a certain limit (the specifications vary from product to product) as it leads to failure. Therefore, this plot helps to choose optimum peak pressure based on the desired corner radius and the maximum allowable thinning for a given component.

Though the pressure path variation has the least effect on thickness at the cup corner, pressure path 2 was found to be the most favorable among the three pressure paths being studied. This can be observed from the main effects plots shown in Figs. 11 and 12. Pressure path 2 results in lowest thinning and lowest corner radius.

4.7 Confirmation tests for minimum thinning and minimum corner radius

Confirmation tests were conducted for the optimum parameters identified from the main effects plot for both the

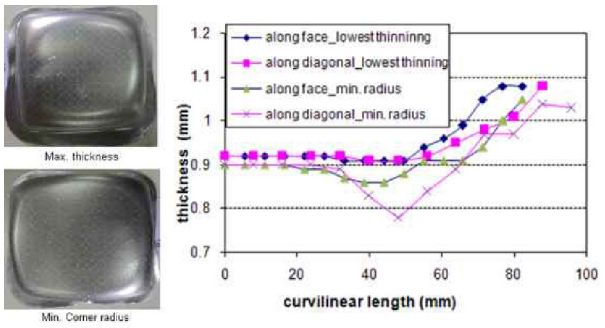

(a) (b)

Fig. 14. Experimental results for minimum thinning (pressure path 2, peak pressure 14.5 MPa and BHF 10 kN) and minimum corner radius (pressure path 2, peak pressure 23.5 MPa and BHF 30 kN): (a) Formed cups; (b) thickness variation.

minimum thickness and the corner radius. Pressure path 2, peak pressure 14.5 MPa and 10 kN BHF were identified (from main effects plot shown in Fig. 11) as process parameters for least thinning at the corner. Optimum process parameters were also identified for the corner radius from the main effects plot (Fig. 12). The minimum corner radius was achieved with peak pressure 23.5 MPa, 30 kN BHF and pressure path 2. The results predicted with these process parameters by regression models and the results from experimental work are in close agreement. The process parameters and the results are summarized in Table 5. Square cups formed with optimum process parameters for lowest thinning (maximum thickness at the corner) and minimum corner radius are shown in Fig. 14(a). It clearly shows better form filling with the parameters identified for the minimum corner radius. The minimum radius is associated with higher thinning, which eventually leads to failure in the corner region.

The thickness variation along the curvilinear length for both the cases are presented in Fig. 14(b) which clearly shows higher thinning in the cup with the minimum corner radius.

5. Conclusions

Based on the results and discussions presented in this paper, the following conclusions are drawn:

(1) Among the three process parameters (pressure path, peak pressure, and blank holding force) studied, the peak pressure is the most significant parameter influencing formability in deep drawing of square cups by hydroforming.

(2) With the experiential setup used in this study, 1 mm thick AA 5182 alloy can be successfully formed into square cups of 100 mm side with a peak pressure up to nearly 24 MPa (without lubrication). Minimum thinning or maximum thickness (0.91 mm) at the corner was achieved with pressure path 2, peak pressure 14.5 MPa and 10 kN blank holding force (BHF). A minimum corner radius of 25.6 mm was achieved with pressure path 2, peak pressure 23.5 MPa and 30 kN BHF.

(3) Pressure path has the least influence on thinning at the corner. However, pressure path 2 results in better formability and form filling as compared to the other two pressure paths. In the case of the corner radius, BHF has the least influence.

(4) With high peak pressure, failure was observed at one of the bottom corners of the cup where biaxial stretching is the predominant mode of deformation during calibration. Thinning in this region was consistently found to be 23-24 % at failure.

(5) The FE simulation predictions of minimum thickness and corner radius are in good agreement with the experimental results. Using the experimental and FEA results, regression equations have been developed for prediction of minimum thickness and corner radius and fitness of the equations was found to be good within the range of process variables used.

References

[1] L. H. Lang, Z. R. Wang, D. C. Kang, S. J. Yuan, S. H. Zhang, J. Danckert and K. B. Nielsen, Hydroforming highlights: sheet hydroforming and tube hydroforming, *J. Mater. Process. Tech.,* 151 (2004) 165-177.

[2] S. K. Singh and D. R. Kumar, Effect of process parameters on product surface finish and thickness variation in hydromechanical deep drawing, *J. Mater. Process. Tech.*, 204 (2008) 169-178.

[3] M. Geiger, M. Merklein and M. Cojutti, Hydroforming of inhomogeneous sheet pairs with counter pressure, *Prod. Eng. Res. Dev.*, 3 (2009) 17-22.

[4] P. Hein and F. Vollertsen, Hydroforming of sheet metal pairs, *J. Mater. Process. Tech.*, 87 (1999) 154-164.

[5] K. Matthias, C. Manfred, T. A. Erman, R. Robert, S. Kerstin and T. Michael, Development of ultra high performance concrete dies for sheet metal hydroforming, *Prod. Eng. Res. Dev.*, 2 (2008) 201-208.

[6] S. Novotny and P. Hein, Hydroforming of sheet metal pairs from aluminum alloys, *J. Mater. Process. Tech.*, 115 (2001) 65-69.

[7] S. H. Zhang and J. Danckert, Development of hydromechanical deep drawing, *J. Mater. Process. Tech.*, 83 (1998) 14-25.

[8] T. Nakagawa, K. Nakagawa and H. Amino, Various applications of hydraulic counter pressure deep drawing, *J. Mater. Process. Tech.*, 71 (1997) 160-167.

[9] E. Onder and A. E. Tekkaya, Numerical simulation of various cross sectional workpieces sing conventional deep drawing and hydroforming technologies, *Int. J. Mach. Tool. Manu.*, 48 (2008) 532-542.

[10] S. G. Desai and P. P. Date, On the quantification of strain distribution in drawn sheet metal products, *J. Mater. Process. Tech.*, 177 (2006) 439-443.

[11] D. Y. Yang, J. B. Kim and D. W. Lee, Investigation into manufacturing of very long cups by hydromechanical deep drawing and ironing with controlled radial pressure, *CIRP Annals*, 44 (1995) 255-258.

[12] M. Sasawat and K. Muammer, Fabrication of microchannel arrays on thin metallic sheet using internal fluid pressure: Investigations on size effects and development of

design guidelines, *J. Power Sources*, 175 (2008) 363-371.
[13] M. H. Hojjati, M. Zoorabadia and S. J. Hosseinipour, Optimization of superplastic hydroforming process of aluminium alloy 5083, *J. Mater. Process. Tech.*, 205 (2008) 482-488.
[14] T. J. Kim, D. Y. Yang and S. S. Han, Numerical modeling of the multi-stage sheet pair hydro forming process, *J. Mater. Process. Tech.*, 151 (2004) 48-53.
[15] H. Z. Shi, X. Z. Li, T. W. Zhong and X. Yi, Technology of sheet hydroforming with a movable female die, *Int. J. Mach. Tool. Manuf.*, 43 (2003) 781-785.
[16] K. P. Rao and J. J. Wei, Performance of a new dry lubricant in the forming of aluminum alloy sheets, *Wear*, 249 (2001) 86-93.
[17] B. H. Lee, Y. T. Keum and R. H. Wagoner, Modeling of the friction caused by lubrication and surface roughness in sheet metal forming, *J. Mater. Process. Tech*., 130-131 (2002) 60-63.
[18] R. Shivpuri and W. Zhang, Robust design of spatially distributed friction for reduced wrinkling and thinning failure in sheet drawing, *Mater. Design*, 30 (2009) 2043-2055.
[19] B. J. Kim, K. H. Choi, K. S. Park, C. J. Van Tyne and Y. H. Moon, Effect of surface defects on hydroformability of aluminum alloys, *Key Eng. Mat.*, 340-341 (2007) 587-592.
[20] B. S. Kang, B. M. Son and J. Kim, A comparative study of stamping and hydroforming processes for an automobile fuel tank using FEM, *Int. J. Mach. Tool. Manu.*, 44 (2004) 87-94.
[21] Y. S. Shin, H. Y. Kim, B. H. Jeon and S. I. Oh, Prototype tryout and die design for automotive parts using welded blank hydroforming, *J. Mater. Process. Tech.*, 130-131 (2002) 121-127.
[22] O. Kreis and P. Hein, Manufacturing system for the integrated hydroforming, trimming and welding of sheet metal pairs, *J. Mater. Process. Tech.*, 115 (2001) 49-54.
[23] M. Geiger, M. Vahl, S. Novotny and S. Bobbert, Process strategies for sheet metal hydroforming of lightweight components, *P. I. Mech. Eng.*, 215/B (2001) 967-976.
[24] W. Liu, G. Liu, X. Cui, Y. Xu and S. Yuan, Formability influenced by process loading path of double sheet hydroforming, *T. NonFerr. Met. Soc.*, 21 (2011) 465-469.
[25] G. Peter and E. Metin, Process control at the sealing line during sheet metal hydroforming, *Prod. Eng. Res. Dev.*, 2 (2008) 3-8.
[26] H. S. Halkaci, M. Turkoz and M. Dilmec, Enhancing formability in hydromechanical deep drawing process adding a shallow drawbead to the blank holder, *J. Mater. Process. Tech.*, 214 (2014) 1638-1646.
[27] A. H. Elkholy and O. M. Al-Hawaj, Collapse pressure and strength analysis of hydroformed circular plates, *Int. J. Adv. Manuf. Technol.*, 18 (2001) 79-88.
[28] M. A. Karkoub, Prediction of hydroforming characteristics using random neural networks, *J. Intel. Manuf.*, 17 (2006) 321-330.
[29] A. Ahmad and R. E. Mohammad, Pressure estimation in the hydroforming process of sheet metal pairs with the method of upper bound analysis, *J. Mater. Process. Tech.*, 209 (2009) 2270-2276.
[30] D. A. Oliveira, M. J. Worswick, M. Finn and D. Newman, Electromagnetic forming of aluminum alloy sheet: Free-form and cavity fill experiments and model, *J. Mater. Process. Tech.*, 170 (2005) 350-362.
[31] A. Nader, P. Farhang and C. John, Forming of AA5182-O and AA5754-O at elevated temperatures using coupled thermo-mechanical finite element models, *Int. J. Plasticity*, 23 (2007) 841-875.
[32] B. Modi and D. R. Kumar, Development of a hydroforming set up for deep drawing of square cups with variable blank holding force technique, *Int. J. Adv. Manuf. Technol.*, 66 (2013) 1159-1169.
[33] D. C. Chen and C. F. Chen, Use of taguchi method to develop a robust design for the shape rolling of porous sectioned sheet, *J. Mater. Process. Tech.*, 177 (2006) 104-108.
[34] M. J. Davidson and K. Balasubramanian, Experimental investigation on flow-forming of AA6061 alloy-A Taguchi approach, *J. Mater. Process. Tech.*, 200 (2008) 283-287.
[35] A. K. Sharma and D. K. Rout, Finite element analysis of sheet hydromechanical forming of circular cup, *J. Mater. Process. Tech.*, 209 (2009) 1445-1453.
[36] B. Modi and D. R. Kumar, Effect of friction and lubrication on formability of AA5182 alloy in hydroforming of square cups, *Mater. Sci. Forum*, 762 (2013) 621-626.
[37] R. Padmanabhan, M. C. Oliveira, J. L. Alves and L. F. Menezes, Influence of process parameters on the deep drawing of stainless steel, *Finite Elem. Anal. Des*., 43 (2007) 1062-1067.
[38] F. Barlat and J. I. Lian, Plastic behavior and stretchability of sheet metals. Part-I: A yield function for orthotropic sheets under plane stress conditions, *Int. J. Plasticity*, 5 (1989) 51-56.
[39] K. P. Rao and C. L. Xie, A comparative study on the performance of boric acid with several conventional lubricants in metal forming processes, *Tribol. Int.*, 39 (2006) 663-668.
[40] M. Javadi and M. Tajdari, Experimental investigation of the friction coefficient between aluminum and steel, *Mater. Sci.*, 24 (2006) 305-310.

Bharatkumar Modi was a research scholar in the Department of Mechanical Engineering, Indian Institute of Technology Delhi, India when this work was carried out. He is presently a Professor of Mechanical Engineering, Nirma University, Ahmedabad, India.

D. Ravi Kumar is a Professor of Mechanical Engineering, Indian Institute of Technology Delhi, India. His research interests include sheet metal forming, finite element analysis, hydroforming, lightweight materials and severe plastic deformation techniques.